Cancer Medicine

WILEY

Cancer Medicine Open Access

RESEARCH ARTICLE OPEN ACCESS

TYRO3, AXL, MERTK and Their Ligands in Brain Metastases From Colorectal Cancers

Anaïs Noblanc[1,2] | Fatima Dkhissi[1] | Pierre-Olivier Guichet[1,2] | Lucie Lebeau[3] | Serge Milin[3] | Sheik Emambux[1,4] | Pauline Roussille[5] | Camille Evrard[1,4] | Lucie Karayan-Tapon[1,2] | David Tougeron[1,6] | Omar Benzakour[1] | Violaine Randrian[1,6]

[1]PRODICET, UR24144, Université de Poitiers, Poitiers, France | [2]Department of Biological Cancerology, CHU de Poitiers, Poitiers, France | [3]Department of Pathology, CHU de Poitiers, Poitiers, France | [4]Department of Oncology, CHU de Poitiers, Poitiers, France | [5]Department of Radiotherapy, CHU de Poitiers, Poitiers, France | [6]Department of Hepatology and Gastroenterology, CHU de Poitiers, Poitiers, France

Correspondence: Violaine Randrian (violaine.randrian@chu-poitiers.fr)

Received: 18 March 2025 | **Revised:** 30 March 2026 | **Accepted:** 15 April 2026

Keywords: AXL | brain metastasis | colorectal cancer | GAS6

ABSTRACT

Introduction: TYRO3, AXL, and MERTK (TAM receptor tyrosine kinases) represent potential therapeutic targets in metastatic colorectal cancer. Pre-clinical and clinical data are needed to explore further how TAM receptors interact with the central nervous system, which could impact brain metastases from colorectal cancer (BM-CRC).

Methods: We analyzed TAM receptor expression in established brain metastasis stem cell lines from patients with CRC (BM-SC-CRC) (RNA and protein), a local cohort of BM-CRC patients (protein), and a cohort of metastatic CRC from The Cancer Genome Atlas (TCGA) (RNA).

Results: When orthotopically injected into mice, BM-SC-CRC derived from two patients expressed TYRO3 and Protein S (PROS1) but poorly AXL and GAS6. When we analyzed both patients' primary tumors and metastatic sites, TYRO3 and AXL proteins were expressed in all tumor sites, but hardly MERTK. AXL was located primarily in endothelial cells, and TYRO3 in tumor cells. We examined the protein expression of TAM receptors in a cohort of BM-CRC patients, considering tissue from the primary tumor ($N = 85$), the matched brain metastases ($N = 40$), and another metastatic site ($N = 29$). AXL was expressed through primary tumors to brain metastases, as 72.7% of samples in BM (versus 44% with TYRO3 and 53% with MERTK) had a stable (45.5%) or increased (27.2%) protein expression compared to their paired primary tumor. None of the TAM receptors or PROS1 were found prognostic in a TCGA metastatic CRC cohort ($n = 80$), but GAS6 was, in univariate (HR = 2.141 [95% CI 1.018–4.506], $p = 0.045$) and multivariate analysis (HR = 2.382 [95% CI 1.124–5.048], $p = 0.024$). In exploratory analysis, patients with Low AXL/High GAS6 had a poorer prognosis ($p = 0.046$).

Discussion and Conclusion: The TAM receptors' ligand GAS6 and the AXL/GAS6 ratio could help to monitor patients' prognosis in metastatic CRC settings including BM-CRC. Further research is needed to validate the TAM receptors' impact on prognosis in BM-CRC.

Omar Benzakour and Violaine Randrian contributed equally to this work and are co-last authors.

1 | Introduction

Unlike brain metastases (BM) from lung cancer or melanoma, BM from colorectal cancer (BM-CRC) are mainly metachronous and of poorer prognosis [1]. This difference in disease history indicates a distinct physiology. BM-CRCs are usually associated with the terminal evolution of CRC, since most BM occur more than 2 years after diagnosis of metastatic CRC. They illustrate a specific aggressiveness acquired over the disease's history, as resistance develops across different treatment lines. Besides, in the Vienna Brain Metastasis registry, brain metastasis from CRC occurs via a unique lesion in more than half of cases (58%). In contrast, it is less frequent in lung (41%) and breast (36%) cancers ($p < 0.05$) [2]. This proportion of unique lesions is also observed in studies of CRC [3–5]. This supports the concept that, unlike breast or lung cancer cells, few CRC cells acquire the properties needed to successfully cross the blood–brain barrier (BBB) and form a specific niche in the brain. Various genes have been identified in primary BM-derived cancers that confer the ability to cross the BBB [6]. These essential data are lacking in the CRC setting. Although identified genes appear to be cancer-specific [6], broad pathways are common to all cancer types. Angiogenesis is an essential mechanism for cancer cell settlement in a distinct environment from its primary site, especially in the brain [7]. Indeed, many drugs and clinical trials in primary brain tumors targeted angiogenesis [8]. However, anti-VEGF therapies showed limited effects on overall survival [8]. There is a need to identify alternative targets in the angiogenic pathway. Moreover, interactions of the cancer cells with the perivascular niche and pre-existing vasculature through endothelial cells, called vascular co-optation, are critical for brain colonization [9].

TAM receptors (TYRO3, AXL, MERTK) and their ligands, Protein S (PROS1) and Growth arrest-specific 6 (GAS6), are particularly interesting as they are both involved in vascular and neural systems [10]. Furthermore, they are explicit in crosstalk between neural stem cells and glioma cells [11–13]. They link to their ligands differently, as TYRO3 and MERTK interact with PROS1 and GAS6, whereas AXL interacts primarily with GAS6 [14]. These differential interactions may have slightly different biological implications for each receptor. MERTK is thought to be expressed in the tumor immune compartment and may exert a controversial effect by promoting inflammation [15]. TYRO3 was stained in polyps and colon cancers and was found to correlate with poor prognosis in colon cancers [16], along with AXL [17]. PROS1 circulates in human plasma at a ~25 μg/mL concentration [18]. PROS1 is also produced at many extrahepatic sites including macrophages [19], vascular endothelial cells (ECs) [20], vascular smooth muscle cells [21], neural stem cells [10], and many cancer cell types [22]. The concentration of Gas6 in human plasma is about 35 ng/mL and may be elevated to about 110 ng/mL in patients with severe sepsis [23]. GAS6 is expressed in the central nervous system [24] and induces neuroinflammation [25]. Both ligands are expressed by antigen-presenting cells [26]. In addition, TAM receptors play a critical role in the phagocytosis of apoptotic cells, thereby modulating the innate immune response [9]. Therefore, targeting TAM receptors may enable disruption of angiogenesis and anti-tumoral immune responses.

Pre-clinical data showed that a combination of AXL inhibitor and immune checkpoint blockade could prolong survival in a glioblastoma model [27]. Pre-clinical data on the pan-TAM small kinase inhibitor RXDX-106 focused on its synergy with immune checkpoint blockade. The authors showed its efficiency in activating effector immune cells and inhibiting tumor growth in vitro and in vivo in a CRC model with microsatellite instability [28]. TAM receptor inhibitors are considered emerging therapeutic agents in metastatic CRC [29, 30]. The tyrosine kinase inhibitor XL092 inhibits AXL, MET (also known as Hepatocyte growth factor receptor), and VEGFR2 (vascular endothelial growth factor receptor 2). XL092, combined with the immune checkpoint inhibitor atezolizumab, was tested against regorafenib in the STELLAR-303 phase III clinical trial (NCT05425940), which includes patients with refractory metastatic CRC [31]. As in many trials, a newly diagnosed untreated brain metastasis is an exclusion criterion.

We aimed to assess whether TAM receptors form therapeutic targets of interest. We focus on BM-CRC patients, an understudied and less well-known CRC subgroup whose cells likely acquired biological characteristics that enable migration into the brain. We used an orthotopic model of BM-CRC stem cells to study the expression of TAM receptors and their ligands. We assessed the protein expression of TAM receptors and their prognostic value in a cohort of patients with BM-CRC. We also evaluated the prognostic potential of RNA expression of TAM receptors and their ligands in a cohort of metastatic CRC patients from TCGA (The Cancer Genome Atlas).

2 | Materials and Methods

2.1 | Patients' Cohort and Tissue Microarray

A part of this study was performed on samples from a previously published cohort of patients with brain metastases from colorectal cancer [1, 32, 33]. Briefly, patients from Poitiers University Hospital, diagnosed with BM-CRC from 2001 to 2016, were identified in the hospital's clinical report database. Inclusion criteria were: age over 18 years, histologically-confirmed CRC, histology- or radiologically-confirmed BM by computed tomography scan and magnetic resonance imaging. As patients were deceased at the time the study was conducted, consent collection was waived. Poitiers University Hospital's Ethics Committee approved the study (DC-2008-565). It was conducted in accordance with the principles of the Declaration of Helsinki.

Patients' biopsies were formalin-fixed and embedded in paraffin for pathological analyses and archiving. Tissue microarray (TMA) blocks were made of four biopsy cores of 1 mm diameter per tumor in the tumor center from each sample (MTA Booster version 1.01; Alphelys, Paris, France) [1]. For each cohort patient, biopsies of the primary tumor, brain, and, if available, non-brain metastases were included in the TMA. The TMA blocks were microsectioned at 3 μm for immunostaining.

2.2 | Stem Cells From Colorectal Cancer Brain Metastasis

Our research team established two colorectal cancer-derived brain metastatic stem cell lines (BM-SC-CRC1 and 2) and

previously described their features [34]. Briefly, colon cancer-derived BM tissue was obtained from two patients undergoing brain tumor resection at the neurosurgery department of the Poitiers University Hospital. These patients gave their written consent before surgery to be included in this protocol, approved by the Poitiers University Hospital's Ethics Committee (DC-2018-3222, *Comité Protection des Personnes CPP Ouest II*). Each tumor sample was mechanically dissociated and cultured in a serum- and antibiotic-free culture medium, allowing neurological stem cell survival (DMEM: F12 [1:1, #31331-028; Gibco], B27 suppl. 0.5X [#17504-044; Gibco], N2 suppl. 0.5X [#17502-048; Gibco], 50 ng/mL FGF-basic [#01-A01110; Isokine], 50 ng/mL EGF [#713008; Biolegend]), at 37°C with a humidified atmosphere of 5% CO_2. After four passages with cell dissociation by Accutase (#A1110501; Gibco) and the formation of metaspheres and/or the proliferation of adherent cells, we considered that the BM-SC-CRC cell line was established. The archived paraffinized tumor biopsies of these two patients were available and microsectioned at 3 μm for further analyses.

As for BM-SC-CRC, their characterization was published [34] before being used for experimentation. Their stable mutational status was authenticated by sequencing upon culture initiation and annually since then. They were tested free from mycoplasma contamination upon culture initiation and regularly, at least annually, since then. Shortly after dissociation and culture, the cell lines formed secondary and tertiary metaspheres, which is a typical stem cell property of self-renewal. In limiting dilution assays, the frequency of metasphere-initiating cells was 2.8%–6.9%. BM-SC-CRCs strongly express CD44, EpCAM, CD133, Lgr5, and ALDH1, which are CRC stem cell markers. They also express CD44V6, which is known to be specifically associated with CSCs presenting metastatic potential in CRC. After a week in culture, BM-SC-CRCs express typical colonic epithelial markers, namely CK20, CK19, and CDX2, showing their differentiation capacity. These cell lines had invasive and migratory capacities in *the in ovo model, with a* 3%–5% metastasis ratio. BM-SC-CRCs could recapitulate brain metastasis in immunocompromised mice when injected orthotopically.

2.3 | Orthotopic Cell Injection

The protocol was approved by the French Ministry of National Education, Higher Education and Research (no. 2018081416455954), and all animal experimental procedures were performed in accordance with the recommendations of the European Union (2010/63/EU) for care and use of laboratory animals and conformed to the ethical guidelines of the French Ministry of Agriculture and Food (Animal Health and Protection Veterinary Service). Both BM-SC-CRC1/2 cells were tested free from mycoplasma contamination before being orthotopically injected into the brain of nude mice to test the tumorigenicity of these cancer stem cells during the study conducted by Desette et al. [34]. Shortly, 1 μL of 10^5 BM-SC-CRC cells in suspension/μL in PBS was injected using a Hamilton syringe with a 27-gauge needle in the striatum (2 mm left and 2.5 mm depth of the bregma) of trepanned 8-week-old female BALB/c nude mice, anesthetized by xylazine/ketamine intravenous injection. Skin clips closed the mice's skin. Mice's health was monitored daily, and a 10% body weight loss in 24 h induced the euthanasia of the animal by a 4% paraformaldehyde intracardiac perfusion, followed by the harvesting of the fixed brain. Tissues were cryosectioned at 5 μm and mounted on 0.5% gelatin-coated SuperFrost Plus microscope slides (VWR).

2.4 | Immunohistochemistry

Immunodetections were performed on the patients' biopsies, TMA paraffinized sections, and the mouse brain tissue sections. First, the paraffinized tissue sections were deparaffinized with Histo-Clear (#64110-01; Electron Microscopy Sciences) and rehydrated, then equilibrated in 1× phosphate-buffered saline (PBS 1×). Antigens were retrieved by the heat-induced method in 10 mM sodium citrate buffer at pH 6.0, and endogenous peroxidases were inhibited (15 min, 3% H_2O_2, diluted in PBS 1×). Tissues were permeabilized for 30 min in PBS 1×, 0.3% Triton X-100, and saturated for 30 min at room temperature with PBS 1×, 3% bovine serum albumin (BSA), 0.1% Triton X-100. The primary antibody was diluted in PBS 1×, 0.3% BSA, 0.1% Triton X-100, and incubated overnight at 4°C before the biotinylated secondary antibody was applied for 30 min at room temperature (dilution at 1/500), followed by 1 μg/mL streptavidin-horseradish peroxidase (#GTX27403; GeneTex). The signal was developed using the Vector ImmPACT DAB peroxidase substrate kit (#SK-4105; Vector Laboratories) according to the manufacturer's instructions, under brightfield microscopic observation (#B-290TB; Optika Microscopes, Italy). The cell nuclei were counterstained for 1 min with a Mayer's Hematoxylin solution (#MHS16; Sigma Aldrich, Merck). Sections were dehydrated by increasing ethanol concentrations and two baths of pure Histo-Clear (#64110-01; Electron Microscopy Sciences) and permanently mounted with Entellan New mounting medium (#1.07961; Millipore, Merck).

Mounted immunostained slides were scanned at a magnification of ×40 with the VS120 virtual slide microscope (Olympus) from the ImageUP microscopy and cytometry analysis facility of the University of Poitiers. Stainings from orthotopic models were read under the supervision of a senior pathologist. TMA stainings were blindly read by two independent scientists, who assigned a semi-quantitative score based on the staining surface. The staining was considered harmful below 10% of positive cancer cells; between 10% and 30%, it was classified as 1; between 30% and 50% of positive cells, it was classified as 2. Stainings in classes 0, 1, and 2 were considered Low. Between 50 and 80% of positive cell staining was classified as 3, and above 80% was classified as 4. Stainings in classes 3 and 4 were considered High. Discordant results were discussed to find consensus.

2.5 | Antibodies

The primary antibodies used in our assays were directed against TYRO3 (rabbit polyclonal; #NBP2-23725; Novus, Bio-Techne; dilution 1:2000), AXL (goat polyclonal; #AF154; R&D Systems, Bio-Techne; 1:400), MERTK (rabbit polyclonal; #MKT-121AP; FabGennix; 1:800), PROS1 (rabbit polyclonal; #A0384; Dako; 1:800), and GAS6 (rabbit polyclonal; generous gift from Dr. Michael Hall [35]; 1:2000). The biotinylated secondary

antibodies were directed against immunoglobulin G from rabbit (donkey polyclonal; #6440-08; SouthernBiotech; 1:500) or from goat (donkey polyclonal; #6425-08; SouthernBiotech; 1:500).

2.6 | RNA Sequencing Analysis

We extracted RNA sequencing data from previous work by Desette et al. [34] published by our laboratory. Briefly, the RNAs were extracted from cells (BM-SC-CRC1/2) cultivated in normal conditions, without treatment, by using the RNeasy Mini Kit (Qiagen) following the manufacturer's protocol and qualified using the Agilent 2100 Bioanalyzer platform (Agilent Technologies). Qualified RNAs were sent to the MGX platform in Montpellier for RNA sequencing. Libraries were produced using a TruSeq Stranded mRNA Sample Preparation Kit (Illumina) and 150 nt paired-end sequenced on a NovaSeq sequencer (Illumina).

The fasta files were deposited in the Sequence Read Archive database (https://www.ncbi.nlm.nih.gov/sra) under the accession number (PRJNA1013918). We compared these data with previous RNA sequencing datasets from four CRC cell lines, corresponding to microsatellite-stable CRC primary tumors (CL40; HT29; LS1034; SW1463), and cultivated under normal conditions without treatment. Raw data were processed using STAR and featureCounts for mapping and counting. Differential expression analysis was performed by using the DESeq2 R package.

2.7 | Statistical Analysis

Descriptive statistics included the median and range for the quantitative variables and frequencies and percentages for qualitative variables. Survival curves were determined using the Kaplan–Meier method, and log-rank tests were used to compare survival outcomes. For cohort analysis, patients were divided into two groups based on immunohistochemical staining for each protein. A staining score of 0, 1, or 2 was considered low. A staining score of 3 or 4 was considered high. The association between overall survival and staining score was examined.

The transcript data from cell lines are based on The Human Protein Atlas version 23.0 (https://www.proteinatlas.org/) and Ensembl version 109 [36, 37]. Clinical and transcriptomic data from patients diagnosed with stage IV-colorectal adenocarcinoma from the TCGA (The Cancer Genome Atlas) cohort were obtained from the cBioPortal for Cancer Genomics (https://www.cbioportal.org/study/summary?id=coadread_tcga_pan_can_atlas_2018). Using TCGA data, patients were classified into two groups based on the RSEM (RNA-seq by expectation–maximization) value for each gene of interest, and the association between overall survival and RSEM was examined. The cut-off was determined as the RSEM value that yields the maximum difference in survival between the two groups at the lowest log-rank *p*-value, using the 'servminer' package in R with a minimum group size of 30% of the cohort.

The significance level was set at a *p*-value of 0.05 (two-sided). Statistical analyses were performed using PRISM 10.1.2 (GraphPad) software, except for the multivariate analyses by Cox regression, which were performed using IBM SPSS Statistics software, version 21.0.0.0.

3 | Results

3.1 | Highly Variable Expression Profile of the TAM Receptors and Their Ligands in Cellular models of Colorectal Cancer

Considering data from the Human Protein Atlas, we found shallow expression of *TYRO3* and *MERTK* in cancer but slightly higher than in non-cancerous tissues (Figure 1A, Figure S1) and a medium to high expression of *AXL* compared to the other genes of the *PROS1*/*TAM* system, but slightly lower than in normal tissues. In CRC, the expression of *TYRO3*, *MERTK*, and *PROS1* is similar to that in most of the other solid tumor tissues; AXL expression is low compared to other solid tumor tissues; GAS6 expression, whereas low compared to non-cancer tissues, is still higher than in most other cancer tissues. *PROS1* is expressed at low levels in cancer, but it can be delivered to cancer cells via the blood/plasma supply, where it is constantly present. *GAS6* expression is lower in cancer tissues than in normal tissues.

When focusing on CRC, *TYRO3*, *AXL*, *MERTK*, and *PROS1* expressions are consistent along the 63 available CRC cell lines, except for seven of them (CaR-1; LS123; MDST8; RKO; SNU-1197, SNU-C5; SW480) in which *AXL* expression is increased (Figure 1B). Overall, the expression profiles of the TAM receptors and PROS1 are consistent across CRC cancer cell lines (Figure 1B). Of note, *GAS6* expression is highly variable between CRC cell lines (no expression: COLO 320DM; HT-29; NCI-H716; high expression: LS513; MDST8; SNU-1033; SW1417), making it hard to determine its level in CRC.

The expression profiles of TAM receptor family members and their ligands differ between BM-SC-CRC cells and CRC cell lines (Figure 1C–G). *TYRO3* is expressed at a level similar to that in other CRC cell lines. Still, *AXL* and *MERTK* are expressed at much lower levels in BM-SC-CRC cells than in other CRC cell lines. As for the ligands, *PROS1* expression is similar across all cell lines, but *GAS6* expression is lower in BM-SC-CRC cells than in different CRC cell lines.

Our lab generated an in vivo model of BM-CRC through orthotopic injection of BM-CRC-derived cell lines from two distinct patients, enriched in stem cells (BM-SC-CRC1 or BM-SC-CRC2) [13]. We assessed proteic expression of TAM receptors and their ligands by immunostaining (Figure 1H–N) in this model. TYRO3 (Figure 1I) is highly expressed at the apical pole of epithelial-like cells. The staining of AXL is hardly detected (Figure 1N). MERTK staining is low in BM-SC-CRC1 tumors and mainly present at the apex of epithelial-like cells in BM-SC-CRC2 tumors (Figure 1J). PROS1 staining is high at the apex of epithelial-like cells in both BM-SC-CRC1/2 tumors (Figure 1K). GAS6 staining is not detected in the BM-SC-CRC2 tumor and at a medium level in epithelial-like cells of the BM-SC-CRC1 tumor (Figure 1L). Under these experimental conditions, PROS1 and GAS6 immunostaining signals and their intensities should be interpreted cautiously, as both GAS6 and PROS1 are secreted, soluble factors. Their detection within cells in brain sections

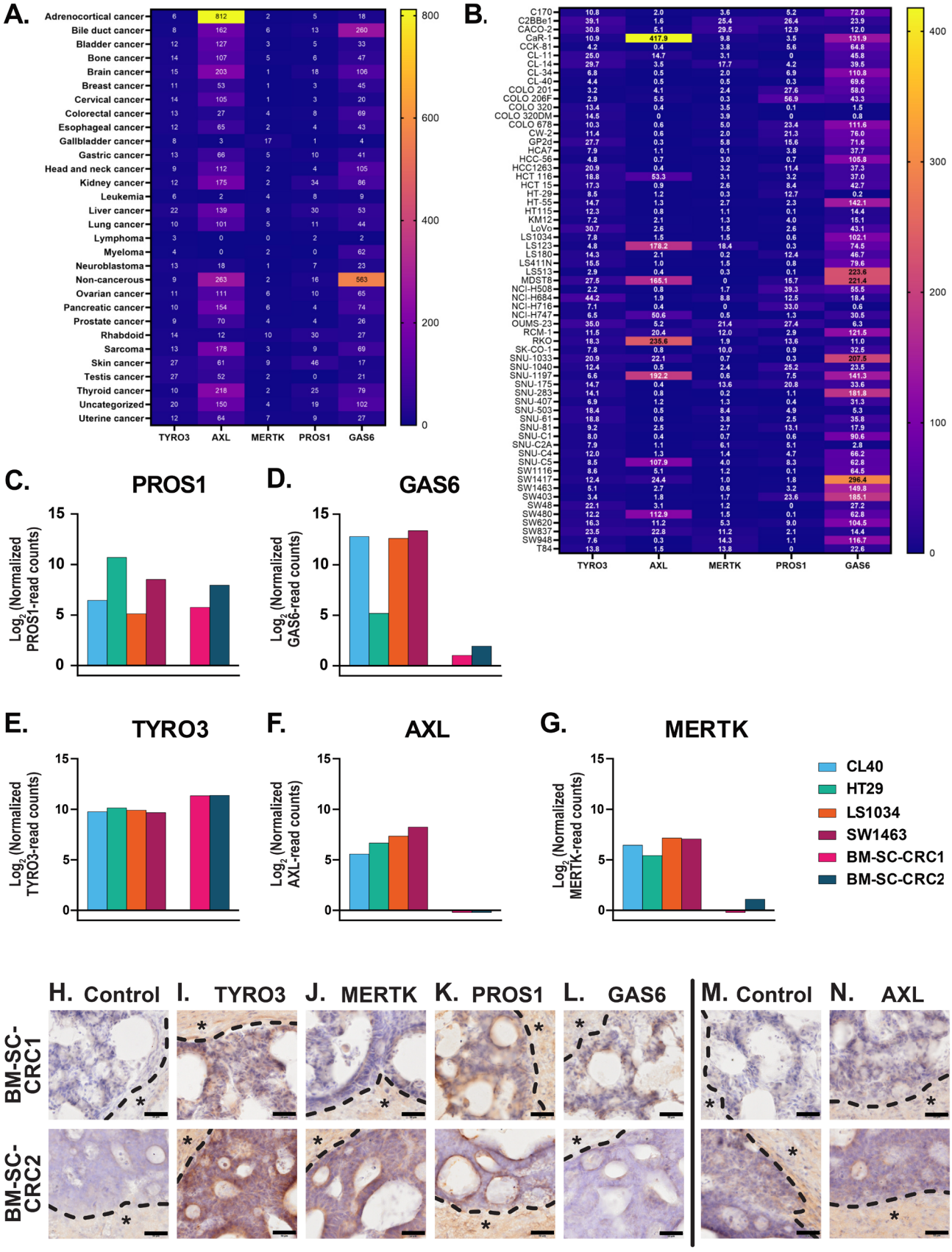

FIGURE 1 | Legend on next page.

FIGURE 1 | TAM receptors and ligands' protein expression profile in in vitro models of CRC and orthotopic in vivo model of BM-CRC. (A) RNAseq data from cell lines presented per cancer type in nTPM (normalized number of transcripts per million) from the Human Protein Atlas database. (B) RNAseq data per colorectal cancer cell line in nTPM from the Human Protein Atlas. (C–G) RNAseq data for PROS1 (C), GAS6 (D), TYRO3 (E), AXL (F), and MERTK (G) in CL40, HT29, LS1034, SW1463, BM-SC-CRC1, and BM-SC-CRC2 cells. (H–N) Nude mouse brains injected with BM-SC-CRC1/2 cells, perfused with 4% PFA, and cut with a microtome (40 μm slices). The control condition (H) is in the absence of a primary antibody showing a unique lesion formed after injection. The red frames correspond to the fields of the higher magnifications (scale bar: Whole brain 2 mm, cropped image 50 μm). Immunostaining for TYRO3 (I), MERTK (J), PROS1 (K) and GAS6 (L) receptors and their ligands (×20 objective, Olympus VS120 slide scanner). The frontier between the human tumor cells and the mouse brain tissue is drawn by a dotted line (*: mouse brain; scale bar: 50 μm). Immunostaining for AXL without (M) and without (N) primary antibody. Scale bar: 50 μm. Nuclei were counterstained in blue.

may either represent an experimental artifact, such as an unspecific signal, or a fraction of these ligands (GAS6 or PROS1) that were synthesized but not yet secreted, or, conversely, were internalized. Regardless of the source of GAS6 or PROS1 signals observed, no definitive conclusions can be drawn about their expression level in the examined brain sections.

3.2 | A Longitudinal Study of TAM Receptor Expression in CRC1/2 Patients Detects TYRO3 and AXL Staining in Differentiated Tumor Tissue

Patient CRC1 underwent a progression of CRC over 6 years from the first diagnosis of the primary tumor without metastasis to the patient's death after the appearance of various metastases, first in the liver, then in the lung, and finally in the brain. Patient CRC2 presented an aggressive CRC, with death occurring only 2 years after the initial diagnosis of the primary tumor. The only metastasis of this patient was found in the brain 1 year after the initial diagnosis. We performed TAM staining on tissue from both patients' primary tumors and metastatic biopsies.

TYRO3 is present at a medium level in the overall tumor in both patients. The intensity and location of the staining did not differ between the primary tumor and the brain tumor in CRC1 (Figure 2B). However, its intensity was higher in the CRC2 BM than in the primary tumor (Figure 2C). Still, it is more concentrated at the apical pole of epithelial-like cells, as indicated by TYRO3 staining in the Human Protein Atlas project. In tissues from CRC1 and 2 (Figure 2B,C), AXL is highly expressed in the endothelial cells of numerous blood vessels (Figure 2, arrows) but is not expressed or expressed at low levels in other cells. MERTK is expressed at a low level in both patients' tissue cells (Figure 2B,C). A close look at those two cases showed a minor variation in TAM protein expression across tumor progression, from the primary tumor to non-brain metastasis and BM. This analysis also complemented the RNAseq data with spatial information, especially regarding AXL, which is expressed in blood vessels rather than in tumor cells within the differentiated tumoral tissue.

3.3 | Staining of AXL Is the Most Reliable of the TAM Receptors From Primary Tumor Tissue to Brain Metastasis

We assessed TAM receptor staining in the METACEB cohort, which has already been published by our group [1, 32, 33]. It gathered 85 patients with BM-CRC, of whom samples from primary tumor tissue were available. Among them, 36.4% were women, and the median age was 64 years (range: 35–85). In this cohort of 85 patients, we could collect and perform stainings on 40 paired samples of primary tumor with brain metastasis and 11 longitudinal samples of primary tumor with brain metastasis and other metastatic sites. The median follow-up time was 41.1 months (1.1–155.3 months).

Staining was not uniform across primary tumors or metastases. TAM stainings were primarily low (0, 1, and 2) in primary tumors: 78.5% for TYRO3 (Figure 3A), 82.9% for AXL (Figure 3B), and 60.0% for MERTK (Figure 3C). The low stainings were persistent in non-brain metastases for TYRO3 (93.1%) and AXL (85.8%), and in half of the cases, 53.6% for MERTK. The proportion of low-staining cells was higher in BM than in primary tumors for MERTK (72.5%) and TYRO3 (87.5%). By contrast, low AXL staining was less frequent in BM (71.8%), suggesting a rebound of AXL staining in BM (Figure 3B). To test this hypothesis, we analyzed the evolution of TAM receptor staining in the available paired samples from primary tumors to brain metastases (Figure 3D). The staining score was either stable or increasing from the primary tumor to BM in about half the samples for TYRO3 (55.9%) and MERTK (53%). Regarding AXL, the staining score was either stable or increasing in 72.7% of the samples. Despite the partial tumor sampling inherent to tissue microarray, the staining confirmed that AXL was mainly, if not exclusively, located in blood vessel walls (Figure 3B, arrows), indicating that it was expressed by endothelial cells. These results suggest that AXL is the most prone TAM receptor to be consistent or increase in the BM compared to the CRC primary tumor. This phenomenon may relate more to angiogenesis in the BM than to tumor cell evolution.

3.4 | GAS6 Is a Prognostic Marker in Metastatic Colorectal Cancer

We extracted TCGA colorectal cancer data from a cohort of patients with metastatic disease, either synchronous or metachronous, classified as stage IV, with a better prognosis than our cohort of BM-CRC. This TCGA cohort comprises 80 patients, among whom 40% are women, with a median age of 59 years (range: 35–87). Primary tumors were mostly colon (71%) with KRAS or NRAS mutation (55%). The median follow-up was 15 months (range: 0.5–82.4). To analyze TAM receptor expression, we determined a cut-off as the RSEM value that yields the maximal difference in survival between the two groups at the lowest log-rank P-value, using the 'servminer' package in R with

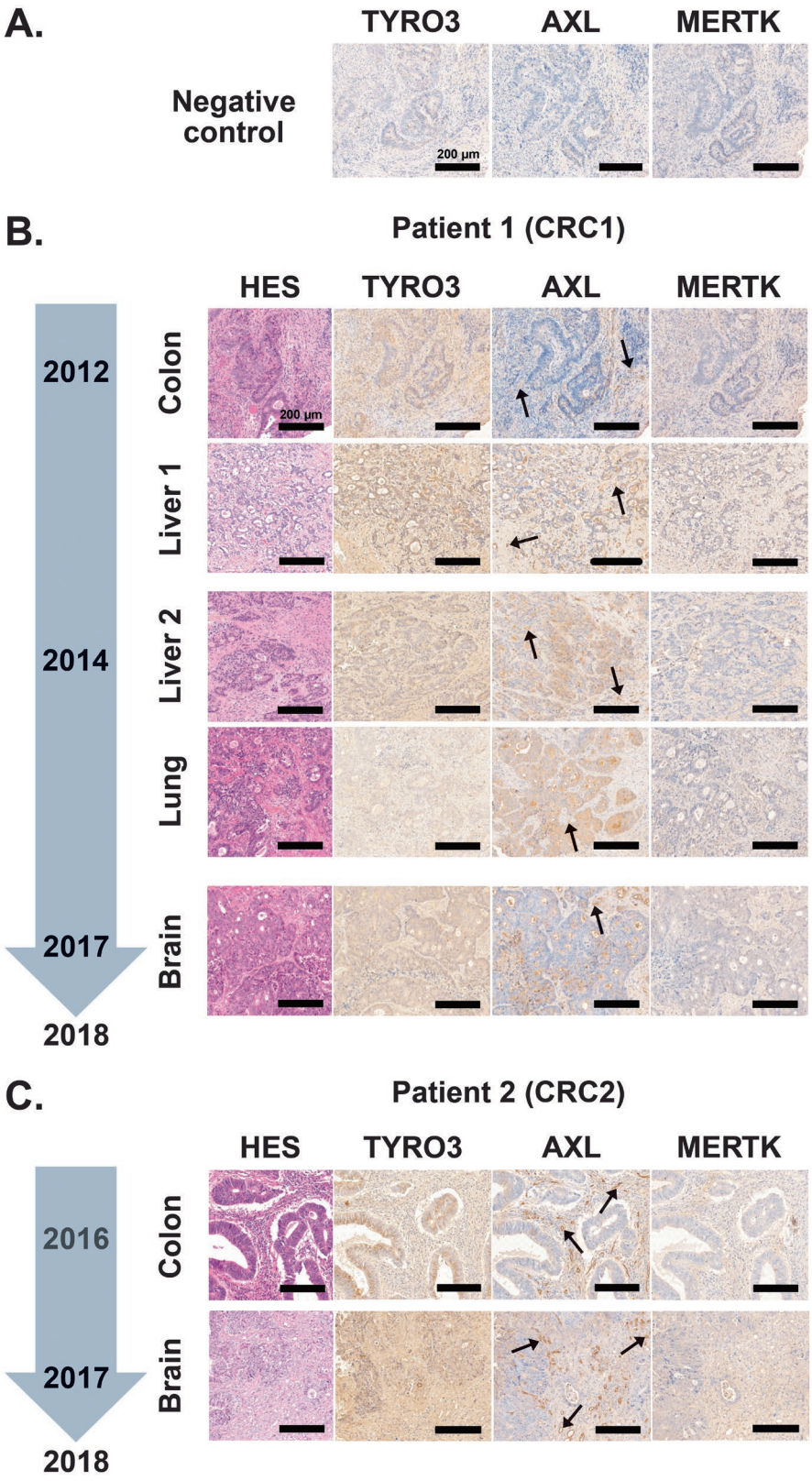

FIGURE 2 | TAM receptors expression profile in tumor tissue of the BM-SC-CRC1/2-issued patients over their clinical history. Fixed and paraffin-embedded tumor biopsies and resected tissues from BM-SC-CRC1/2-issued patients were stained with hematoxylin/eosin (HES) or immunostained (brown) for the TAM receptors. Nuclei were counterstained in blue (scale bar: 200 µm; Olympus VS120 slide scanner). (A) Negative control without primary antibody on patients' tissues. (B, C) Representative images of the stained tissues from patients 1 (B) and 2 (C). Arrows highlight blood vessels. Scale bar: 200 µm.

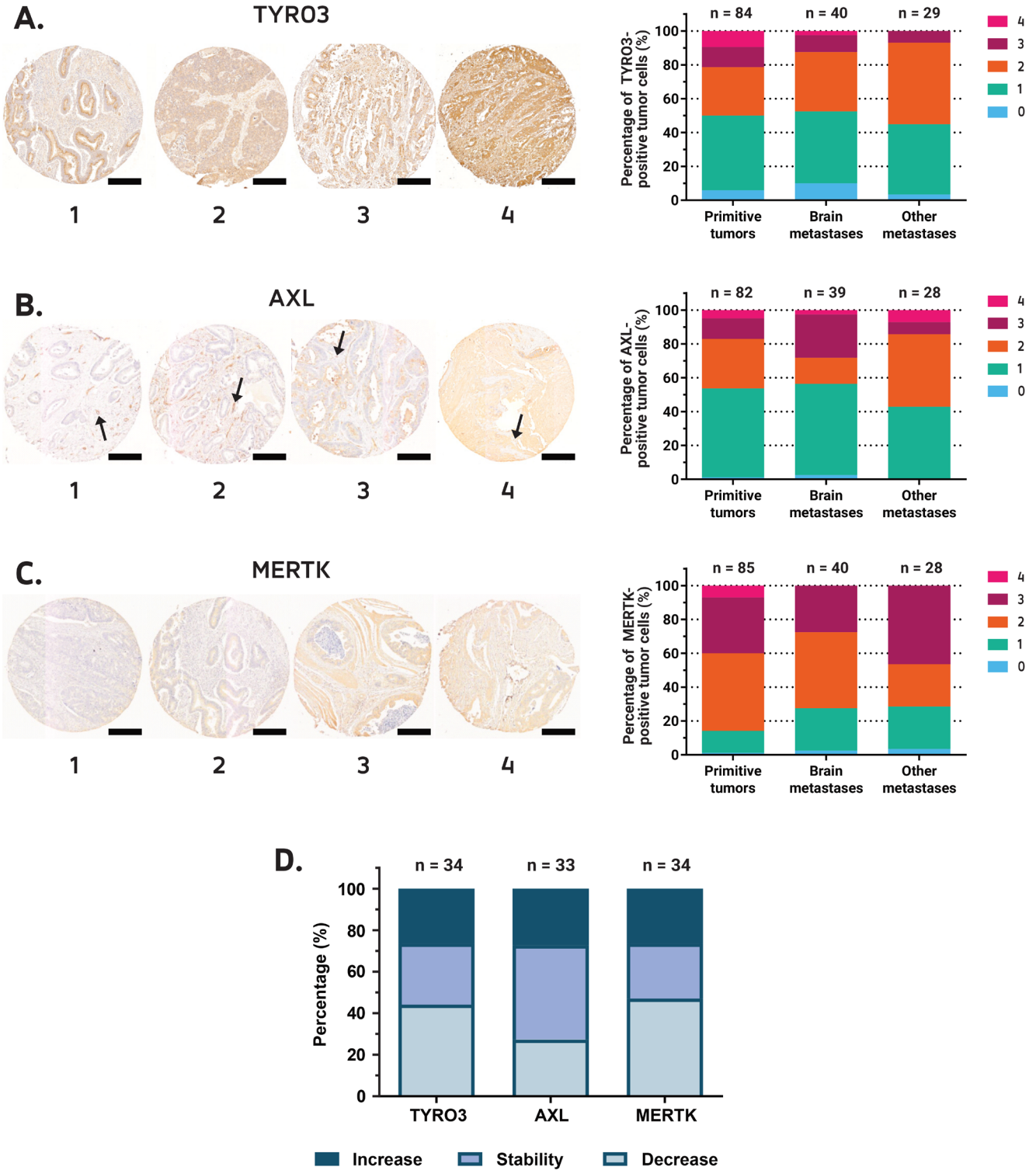

FIGURE 3 | TAM receptors are expressed in a cohort of CRC patients with BM. Three micrometer paraffin slices of a tissue micro-array from a cohort of 87 patients with CRC were immunostained for TYRO3, AXL, and MERTK ($n = 87$, including $n = 37$ with BM; [37–39]; blue Mayer's hematoxylin counterstaining). (A–C) Immunostaining scores were assigned from 1 to 4, according to the percentage of positive tumor cells, as shown in these representative images of TYRO3 (A), AXL (B), and MERTK (C) staining in biopsies from the tumor center. Arrows highlight blood vessels (scale bar: 300 μm; ×20 magnification on Olympus VS120 slide scanner). (D) Evolution of the immunostaining score from the primary tumor to the BM.

a minimum group size of 30% of the cohort. In univariate analysis (Table 1), despite a trend for MERTK, no TAM receptors were statistically associated with OS, nor was PROS1. A high level of GAS6 was associated with a prolonged OS (HR = 2.141 [95% CI 1.018–4.506], $p = 0.045$). Age above 65 years (HR = 3.023 [95% CI 1.393–6.557], $p = 0.005$) was prognostic, as expected. In multivariate analysis, only the variables significantly associated with OS were included in the model. Age above 65 years

TABLE 1 | Univariate and multivariate analysis of known prognostic factors and TAM receptors and their ligands expression in patients with metastatic colorectal cancer in The Cancer Genome Atlas.

			Overall survival			
			Univariate analysis		Multivariate analysis	
Variables	**Conditions**	***n***	**Hazard ratio (95% CI)**	***p***	**Hazard ratio (95% CI)**	***p***
Age	> 65	40	3.023 (1.393–6.557)	0.005	3.122 (1.432–6.809)	0.004
	≤ 65	40				
Sex	Female	33	1.148 (0.569–2.315)	0.700		
	Male	47				
T stage	T2/T3	54	0.474 (0.219–1.023)	0.057		
	T4	25				
N stage	N0	10	1.764 (0.666–4.675)	0.253		
	N1/N2	70				
Synchronicity	No	71	1.019 (0.353–2.946)	0.972		
	Yes	9				
Primary tumor origin	Colon	57	2.335 (0.893–6.085)	0.083		
	Rectum	23				
Microsatellite stability	MSI	2	1.663 (0.222–12.446)	0.620		
	MSS	67				
K/N-RAS mutations	Mutated	38	1.439 (0.678–3.054)	0.343		
	WT	31				
RAS-BRAF mutations and/or ERBB2 amplifications	Mutated	41	1.570 (0.733–3.360)	0.246		
	WT	29				
Aneuploidy score	≥ Median	36	0.608 ()0.294–1.255	0.179		
	< Median	43				
TYRO3 mRNA	High	45	0.746 (0.374–1.486)	0.404		
	Low	35				
AXL mRNA	High	29	0.509 (0.235–1.103)	0.087		
	Low	51				
MERTK mRNA	High	48	0.506 (0.255–1.004)	0.051		
	Low	32				
PROS1 mRNA	High	24	0.550 (0.246–1.229)	0.145		
	Low	56				
GAS6 mRNA	High	42	2.141 (1.018–4.506)	0.045	2.227 (1.055–4.700)	0.036
	Low	38				

Note: N, lymph node; *Sync*, synchronous metastases; T, tumor.

(HR = 3.122 [95% CI 1.432–6.809], $p = 0.004$) and a high level of GAS6 (HR = 2.227 [95% CI 1.055–4.700], $p = 0.036$) remained independent factors for prolonged OS.

3.5 | The Ligand-Receptor Balance Between AXL and GAS6 Impacts Prognosis

As an exploratory analysis, we assessed in the TCGA cohort whether the association of GAS6 with prognosis differed. Of the three TAM receptors, only the combination of AXL and GAS6 levels could discriminate between patients (Figure 4A–C). Patients with Low AXL/High GAS6 had a shorter median OS of 20 months ($p = 0.046$). Patients with Low AXL/Low GAS6 and High AXL/High GAS6 had an intermediate prognosis with a median OS of 33 months. Patients with High AXL/Low GAS6 had a prolonged median OS of 44 months. These results highlight that AXL availability for GAS6 binding is critical for the prognosis of metastatic CRC.

3.6 | BM Stainings Better Stratify BM-CRC Patients Than Primary Tumor Stainings

In our BM-CRC cohort, we assessed the prognostic value of TAM receptors based on their staining scores in primary tumor tissue.

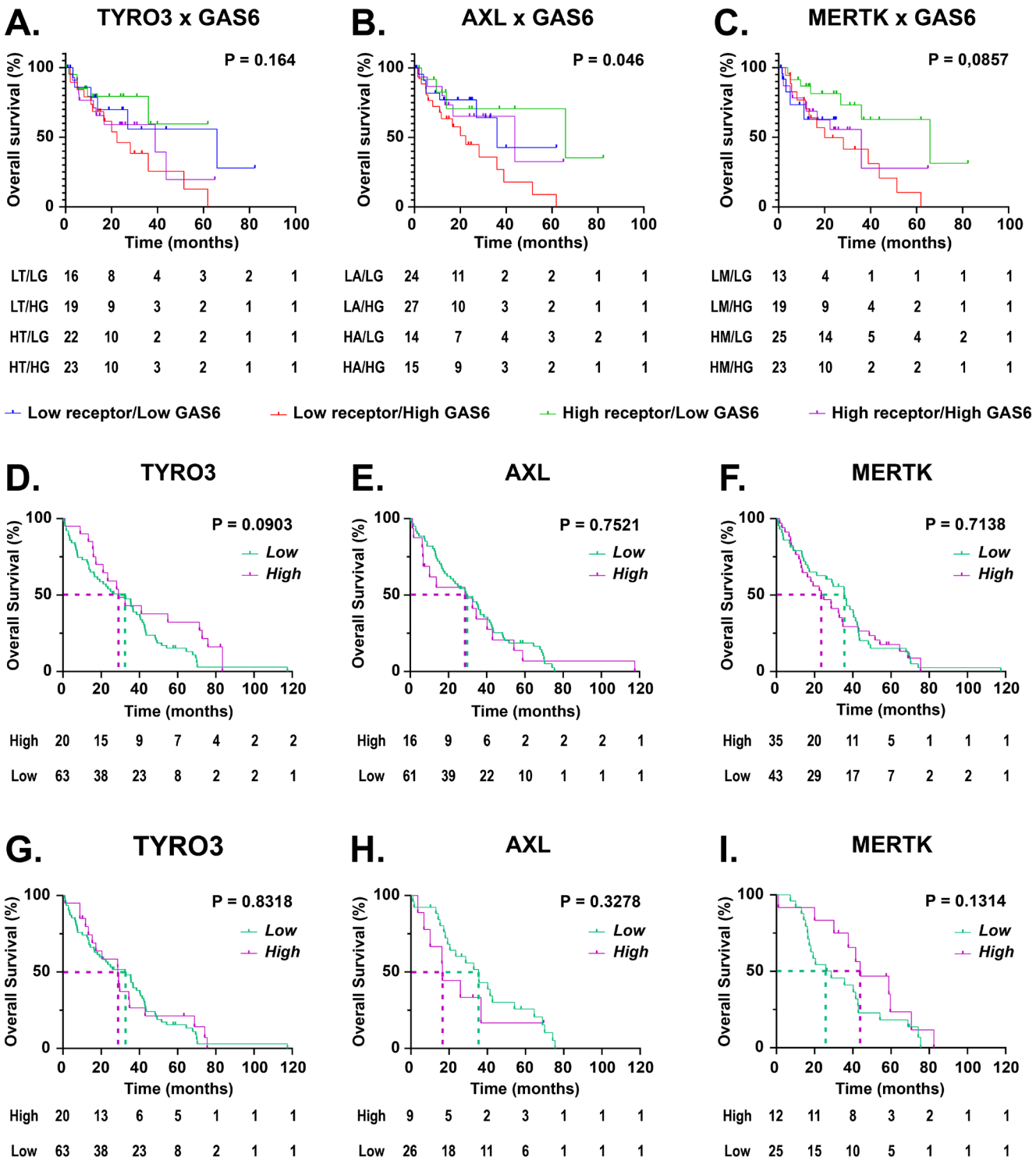

FIGURE 4 | Prognostic value of TAM receptors in mCRC TCGA and BM-CRC cohorts. Kaplan–Meier survival curves (A–C). TAM in the TCGA cohort of 85 patients with metastatic disease upon diagnosis. OS is defined as the time from primary tumor diagnosis. Patients were split according to the RNA expression level in the tumor (RSEM) into Low or High. Overall survival depending on the combined expression of TYRO3-GAS6 (A), AXL-GAS6 (B), MERTK-GAS6 (C). (D–F) In the BM-CRC cohort, patients were split according to the staining score in immunohistochemistry into Low (0, 1, 2) or High (3, 4). OS is the time from metastatic disease diagnosis; TYRO3 in the primary tumor (D), AXL in the primary tumor (E), MERTK in the primary tumor (F). (G–I) TYRO3 in BM (G), AXL in BM (H), MERTK in BM (I).

We split the cohort into tumors with low (0, 1, 2) or high (3, 4) staining scores. When defining overall survival (OS) from the time of metastatic disease diagnosis (stage IV) (Figure 4D–F), TAM receptors did not stratify the patient cohort, consistent with TCGA data primarily obtained from primary tumors. When analyzing the BM stainings (Figure 4G–I), TAM receptors were not prognostic, whereas AXL and MERTK showed distinct OS curves. Patients with Low MERTK had a shorter median OS of

29 months, whereas those with High MERTK had a median OS of 43 months. Although not statistically significant, we observed the most clinically relevant difference in AXL data: patients with Low AXL had a median OS of 16 months, and those with High AXL had a median OS of 35.4 months.

4 | Discussion

Our work dissected the expression of TAM receptors and their ligands in different models of metastatic CRC. Orthotopic in vivo models of BM-CRC, enriched in stem cells, showed TYRO3 staining, primarily in epithelial-like cells. AXL staining was especially low in that model. Consistently, in both BM-SC-CRC1 and BM-SC-CRC2, whereas TYRO3 and PROS1 were expressed, AXL, MER, and their ligand GAS6 were hardly detected by RNA sequencing. Considering CRC-differentiated cell lines, TAM receptors and their ligands are differentially expressed. Tracking back in patients CRC1 and CRC2, TYRO3 and AXL were detectable in primary tumor tissue, whereas MERTK was hardly detectable. AXL protein expression predominates in blood vessels over tumor cells throughout the analyzed primary and metastatic tumor tissues. Turning to the BM-CRC cohort, although not expressed in all patients, AXL is the marker with the most stable or increased cases from the primary tumor to the BM. RNA expression of the TAM receptors did not correlate with overall survival in a TCGA cohort of metastatic CRC. RNA expression of the TAM ligand, GAS6, was an independent prognostic factor in this metastatic CRC cohort. Further analysis showed a statistically significant shortened OS in patients with low AXL and high GAS6. AXL staining was not prognostic in our BM-CRC cohort, but it showed better OS discrimination in BM tissue (Figure 5).

In Desette et al. [34], the transcriptomic analysis of the cell lines reported had a common invasiveness signature of 43 genes. These data lead us to consider the BM-SC-CRC used in our study representative of BM-SC-CRCs. The stem cell frequency was 3%–9% in BM-SC-CRC1 and 7%–13% in BM-SC-CRC2 which is an enrichment compared to the stem cell fraction in organoid models of primary or mCRC, ranging from 0.04% to 1.8% [38]. However, this frequency remains low and does not discard the classical metastatic adaptation. Therefore, this enrichment in stem cells does not account for the low expression of AXL, MERTK, and GAS6 in BM-SC-CRC1 and BM-SC-CRC2. Control cell lines were CL40, HT29, LS1034, and SW1463, which were immortalized from locally advanced colorectal cancer. The late metastatic stage of patients whose BM-SC-CRC1 and BM-SC-CRC2 were developed could account for the discrepancies in TAM receptors. However, positive staining in patients' tissue indicates that TAM receptors were expressed in the original tumor. AXL was primarily detected in endothelial cells from patients' samples, whereas TYRO3 was detected in epithelial colon cancer cells. MERTK is expressed in leukocytes rather than epithelial cells. As we could not observe any vascular structure in the obtained orthotopic tumor, this may account for the absence of AXL and MERTK. These data suggest that, in our BM-SC-CRC models, AXL is predominantly expressed in endothelial cells rather than epithelial tumor cells. Therefore, they would appear later in metastasis, when tumor cells established a crosstalk with their microenvironment and started angiogenesis. A model that incorporates vascular differentiation by culturing cell lines in a medium enriched with vascular growth factors would enable better characterization of TAM receptors in a BM-CRC setting.

Among ligands, PROS1 was similarly expressed across all cell lines; GAS6 showed deficient expression in BM-SC-CRC1 and BM-SC-CRC2, and RNA expression was consistent with protein detection. These discrepancies in ligand expression are consistent with the literature, as PROS1 and GAS6 seem to be provided by different sources. PROS1 was found in tumor cells in an oral squamous cell carcinoma model [39], whereas GAS6 was presented to tumor cells by tumor leukocytes [40]. The expression of PROS1 and TYRO3 throughout different cell lines, including BM-SC-CRC1 and 2, suggests they are critical for the stem cell niche. Conversely, GAS6 expression may rise upon cell differentiation and be provided by the tumor microenvironment. It has long been known that GAS6 is widely expressed in the central nervous system [26, 35], and it is part of the microglial signature, along with PROS1 and MERTK [41]. Recently, a group showed that, compared with the liver, the brain expressed GAS6 at higher levels, particularly in microglia [42]. This reinforces the hypothesis of a tight crosstalk between metastatic tumor cells and the brain niche.

TAM receptors, especially AXL, have emerged as potential therapeutic targets [29–31, 42–46] that target both angiogenesis and immunity. TAM inhibition has been achieved with a multi-target molecule, XL092, also known as zanzalintinib. Its preclinical validation included testing on colorectal cancer cell lines [46] and a phase I trial in solid tumors (STELLAR-002; NCT05176483), showing the feasibility of drug administration [47]. The phase III trial in metastatic CRC [31] showed significantly prolonged median overall survival (mOS) in patients treated with zanzalintinib and atezolizumab as compared to regorafenib: stratified hazard ratio (HR) 0.80 (95% CI 0.69–0.93); $p = 0.0045$ with mOS = 10.9 months (95% CI 9.9–12.1) versus 9.4 months (8.5–10.2). This effect was increased in patients without liver metastases (HR = 0.79 [95% CI 0.61–1.03]; $p = 0.087$; mOS = 15.9 months [95% CI 13.5–17.6] vs. 12.7 months [10.9–15.5]). As in many trials, patients with brain metastases were excluded. Our results show that AXL staining was stable or increased from the primary tissue to the BM. Further datasets are necessary to establish the correlation between AXL expression and response to TAM inhibitors. Data obtained from immunohistochemistry may require RNAseq confirmation and would allow exploration of the AXL-GAS6 ligand-receptor ratio in tumor tissue.

As for the prognostic potential of TAM receptor RNAseq expression, it failed to stratify the TCGA metastatic CRC cohort, whereas high GAS6 expression was an independent prognostic factor for prolonged OS in multivariate analysis. More specifically, the combination of high GAS6 expression and low AXL expression was associated with shorter OS, suggesting that the availability of AXL domains for GAS6 ligand binding is crucial. This data highlights the importance of considering both receptors and ligands when stratifying patients and underscores AXL's role as a limiting factor. TYRO3 was found to be prognostic in an all-comer cohort of patients with CRC [16]. Our results

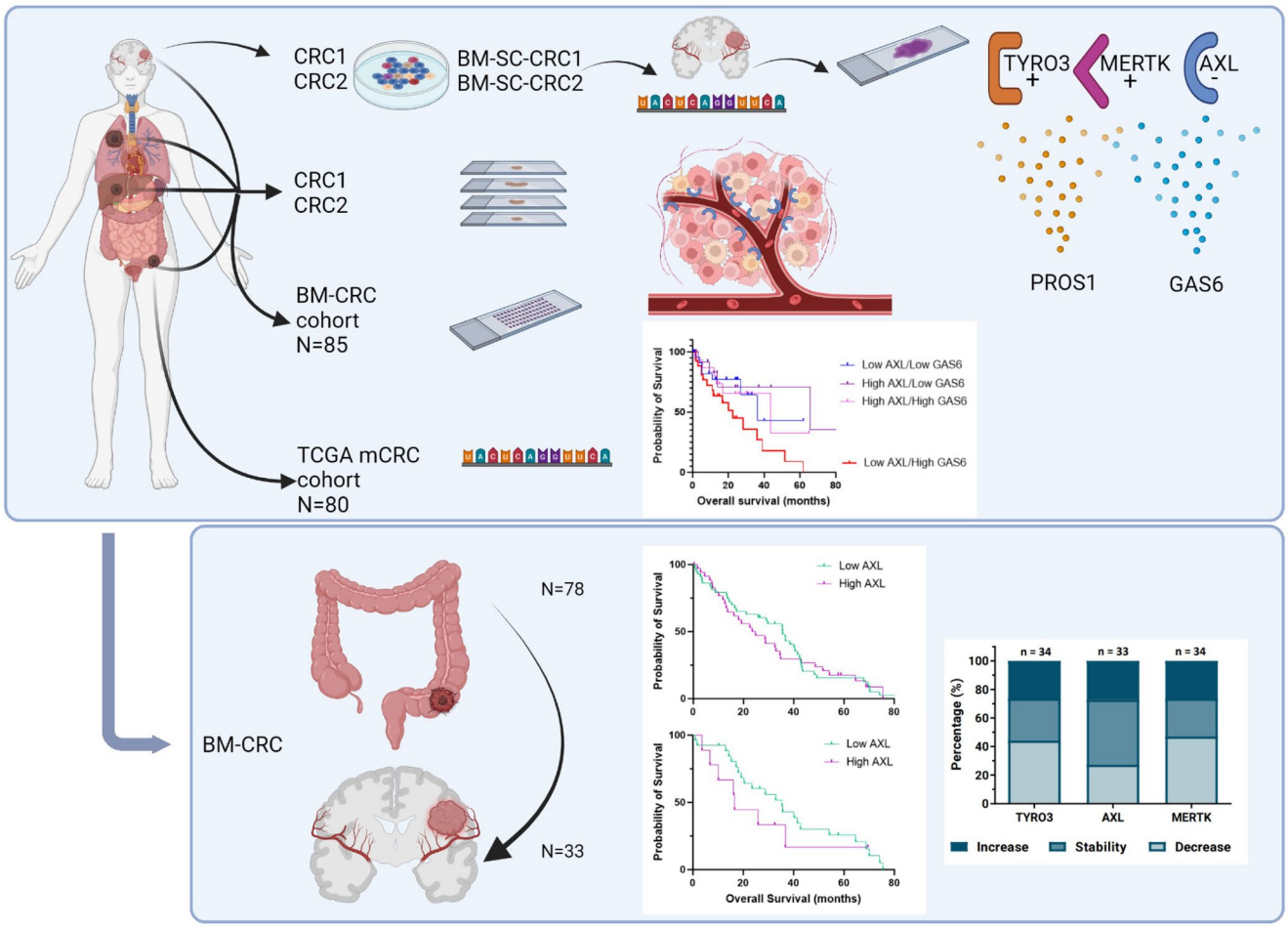

FIGURE 5 | Graphical abstract. TAM receptors and their ligands in brain metastases from colorectal cancers. We assessed TAM receptors in different models. Created with Biorender.com. First, stem-cell enriched BM-derived cell lines from two CRC patients, CRC1 and CRC2. Orthotopic BM mice model and RNAseq data were generated, showing that AXL and its ligand GAS6 were poorly expressed in those stem-cell enriched models. Second, we stained for TAM receptors on tissues from the primary tumor and metastatic sites in CRC1 and CRC2 patients, discovering that AXL was expressed in those tissues but on endothelial cells. TYRO3 was instead expressed on tumor cells and MERTK on leukocytes. Third, we stained for TAM receptors in a tissue micro-array of primary tumor, non-brain, and brain metastases from a local cohort of 85 patients. This confirmed the vascular location of AXL and showed the evolution of TAM protein expression from primary tumor to BM tissue. Last, we studied the prognostic properties of TAM receptors and their ligand in a TCGA cohort of patients with metastatic CRC. GAS6 appeared as a robust prognostic factor and suggested a prognostic impact of the balance between AXL and GAS6 expression as patients with tumors expressing Low AXL/High GAS6 had a significantly shortened overall survival. Finally, we provide a comprehensive study of TAM expression in metastatic CRC with a strong focus on BM-CRC, underlining AXL expression evolution from primary tumor to BM and its prognostic potential in BM-CRC. Although non-significant, AXL proteic expression stratifies better the patients with BM-CRC when assessed in brain tissue instead of primary tumor tissue. AS compared with TYRO3 and MERTK, AXL proteic expression is more frequently conserved, meaning increased or stable, from primary tumor to brain metastasis.

do not contradict this publication as we focused on metastatic CRC. Noteworthy, there was a non-significant trend of longer OS in patients with high MERTK expression. The combination of MERTK expression with GAS6 expression did not stratify the cohort. This aligns with its controversial biological properties, which promote inflammation and maintain the blood–brain barrier [48]. It was established that GAS6 has a much higher affinity for AXL than for TYRO3 and MERTK [49], which also bind PROS1. Studies in mice models suggested that AXL and MERTK deficiency promoted colon tumorigenesis [15] and GAS6 [50]. Here, we generated human data from the TCGA metastatic CRC cohort and our BM-CRC cohort, showing that a single TAM receptor was not a prognostic factor. The TCGA data highlight the prognostic role of GAS6 and the AXL-GAS6 couple in metastatic CRC, which was not established in the BM-CRC cohort.

This study has limitations: the cell lines derived from BM-CRC patients did not reproduce the TAM receptor status of the original tissue. This shows the critical input of studies directly conducting on patient tissues. Regarding patient data, the number of samples in the BM-CRC, especially the number of matched primary tumor and BM tissue samples, may limit statistical power. Therefore, validation in an independent cohort would strengthen our findings. Then, the sample's age makes reliable RNA extraction impossible. Although our immunohistochemical assessment provides spatial information, it may be less sensitive than RNA sequencing. However, the finding in the TCGA

cohort that none of the TAM receptors are prognostic, whereas we can find other robust prognostic factors, strengthens our conclusions. A finely tuned AXL-GAS6 pathway appears essential for monitoring patients' prognosis and may affect the efficacy of TAM inhibitors.

5 | Conclusion

TAM receptors and their ligands were detected in various CRC cell lines and tissues, including the brain, but AXL and GAS6 were absent in stem cell-enriched models. In metastatic CRC patient data, high RNA expression of GAS6 is an independent prognostic factor as it is associated with longer OS and, in exploratory analysis, the combination of Low AXL-High GAS6 appears to be of poor prognosis. Further research to explore the biological availability of AXL towards GAS6 in the specific BM-CRC micro-environment is required to assess its impact on prognosis and the potential of anti-TAM therapies.

Author Contributions

A.N. design of the work, acquisition, analysis, and interpretation of data, writing of the manuscript. F.D. conception of the work, review of the manuscript. P.-O.G. acquisition, analysis, and interpretation of data. L.L. acquisition, analysis, and interpretation of data. S.M. analysis and interpretation of data. P.R. acquisition of data. S.E. acquisition of data. L.K.-T. conception of the work, review of the manuscript. D.T. conception of the work, review of the manuscript. O.B. conception of the work, review of the manuscript. V.R. conception and design of the work, acquisition, analysis, and interpretation of data, writing of the manuscript.

Funding

This study was funded by Sports and Collection 2020.

Ethics Statement

Poitiers University Hospital's Ethics Committee approved the study (DC-2008-565). It was conducted in accordance with the principles of the Declaration of Helsinki.

Consent

Written informed consent was collected for all patients included in the study.

Conflicts of Interest

The authors declare no conflicts of interest.

Data Availability Statement

The datasets supporting the conclusions of this article are available in the Sequence Read Archive database, under the accession number (PRJNA1013918): https://www.ncbi.nlm.nih.gov/bioproject/PRJNA1013918. The corresponding author will provide data from the BM-CRC cohort upon reasonable request.

References

1. P. Roussille, G. Tachon, C. Villalva, et al., "Pathological and Molecular Characteristics of Colorectal Cancer With Brain Metastases," *Cancers* 10, no. 12 (2018): 504, https://doi.org/10.3390/cancers10120504.

2. A. Steindl, T. J. Brunner, K. Heimbach, et al., "Changing Characteristics, Treatment Approaches and Survival of Patients With Brain Metastasis: Data From Six Thousand and Thirty-One Individuals Over an Observation Period of 30 Years," *European Journal of Cancer* 162 (2022): 170–181, https://doi.org/10.1016/j.ejca.2021.12.005.

3. C. Nieder, M. Hintz, and A. L. Grosu, "Predicted Survival in Patients With Brain Metastases From Colorectal Cancer: Is a Current Nomogram Helpful?," *Clinical Neurology and Neurosurgery* 143 (2016): 107–110, https://doi.org/10.1016/j.clineuro.2016.02.022.

4. C. Nieder, A. Pawinski, and L. Balteskard, "Colorectal Cancer Metastatic to the Brain: Time Trends in Presentation and Outcome," *Oncology* 76, no. 5 (2009): 369–374, https://doi.org/10.1159/000210026.

5. M. L. Shindorf, M. S. Jafferji, and S. L. Goff, "Incidence of Asymptomatic Brain Metastases in Metastatic Colorectal Cancer," *Clinical Colorectal Cancer* 19, no. 4 (2020): 263–269, https://doi.org/10.1016/j.clcc.2020.09.002.

6. J. Fares, D. Kanojia, A. Rashidi, I. Ulasov, and M. S. Lesniak, "Genes That Mediate Metastasis Across the Blood–Brain Barrier," *Trends Cancer* 6, no. 8 (2020): 660–676, https://doi.org/10.1016/j.trecan.2020.04.007.

7. D. R. Bielenberg and B. R. Zetter, "The Contribution of Angiogenesis to the Process of Metastasis," *Cancer Journal* 21, no. 4 (2015): 267–273, https://doi.org/10.1097/PPO.0000000000000138.

8. B. K. Ahir, H. H. Engelhard, and S. S. Lakka, "Tumor Development and Angiogenesis in Adult Brain Tumor: Glioblastoma," *Molecular Neurobiology* 57, no. 5 (2020): 2461–2478, https://doi.org/10.1007/s12035-020-01892-8.

9. P. García-Gómez and M. Valiente, "Vascular Co-Option in Brain Metastasis," *Angiogenesis* 23, no. 1 (2020): 3–8, https://doi.org/10.1007/s10456-019-09693-x.

10. G. Lemke, "Biology of the TAM Receptors," *Cold Spring Harbor Perspectives in Biology* 5, no. 11 (2013): a009076, https://doi.org/10.1101/cshperspect.a009076.

11. A. Gely-Pernot, V. Coronas, T. Harnois, et al., "An Endogenous Vitamin K-Dependent Mechanism Regulates Cell Proliferation in the Brain Subventricular Stem Cell Niche," *Stem Cells* 30, no. 4 (2012): 719–731, https://doi.org/10.1002/stem.1045.

12. A. Ginisty, A. Gély-Pernot, L. Abaamrane, et al., "Evidence for a Subventricular Zone Neural Stem Cell Phagocytic Activity Stimulated by the Vitamin K-Dependent Factor Protein S," *Stem Cells* 33, no. 2 (2015): 515–525, https://doi.org/10.1002/stem.1862.

13. A. Ginisty, L. Oliver, P. Arnault, F. Vallette, O. Benzakour, and V. Coronas, "The Vitamin K-Dependent Factor, Protein S, Regulates Brain Neural Stem Cell Migration and Phagocytic Activities Towards Glioma Cells," *European Journal of Pharmacology* 855 (2019): 30–39, https://doi.org/10.1016/j.ejphar.2019.04.039.

14. N. Al Kafri, J. Ahnström, A. Teraz-Orosz, et al., "The First Laminin G-Like Domain of Protein S Is Essential for Binding and Activation of Tyro3 Receptor and Intracellular Signalling," *Biochemistry and Biophysics Reports* 30 (2022): 101263, https://doi.org/10.1016/j.bbrep.2022.101263.

15. L. Bosurgi, J. H. Bernink, V. Delgado Cuevas, et al., "Paradoxical Role of the Proto-Oncogene Axl and Mer Receptor Tyrosine Kinases in Colon Cancer," *Proceedings of the National Academy of Sciences* 110, no. 32 (2013): 13091–13096, https://doi.org/10.1073/pnas.1302507110.

16. C. W. Chien, P. C. Hou, H. C. Wu, et al., "Targeting TYRO3 Inhibits Epithelial–Mesenchymal Transition and Increases Drug Sensitivity in Colon Cancer," *Oncogene* 35, no. 45 (2016): 5872–5881, https://doi.org/10.1038/onc.2016.120.

17. P. D. Dunne, D. G. McArt, J. K. Blayney, et al., "AXL Is a Key Regulator of Inherent and Chemotherapy-Induced Invasion and Predicts a

Poor Clinical Outcome in Early-Stage Colon Cancer," *Clinical Cancer Research* 20, no. 1 (2014): 164–175, https://doi.org/10.1158/1078-0432.CCR-13-1354.

18. B. Dahlbäck, "The Tale of Protein S and C4b-Binding Protein, a Story of Affection," *Thrombosis and Haemostasis* 98, no. 7 (2007): 90–96.

19. D. Lumbroso, S. Soboh, A. Maimon, S. Schif-Zuck, A. Ariel, and T. Burstyn-Cohen, "Macrophage-Derived Protein S Facilitates Apoptotic Polymorphonuclear Cell Clearance by Resolution Phase Macrophages and Supports Their Reprogramming," *Frontiers in Immunology* 9 (2018): 358, https://doi.org/10.3389/fimmu.2018.00358.

20. D. S. Fair, R. A. Marlar, and E. G. Levin, "Human Endothelial Cells Synthesize Protein S," *Blood* 67, no. 4 (1986): 1168–1171.

21. O. Benzakour and C. Kanthou, "The Anticoagulant Factor, Protein S, Is Produced by Cultured Human Vascular Smooth Muscle Cells and Its Expression Is Up-Regulated by Thrombin," *Blood* 95, no. 6 (2000): 2008–2014.

22. N. Al Kafri and S. Hafizi, "Tumour-Secreted Protein S (ProS1) Activates a Tyro3-Erk Signalling Axis and Protects Cancer Cells From Apoptosis," *Cancers* 11, no. 12 (2019): 1843, https://doi.org/10.3390/cancers11121843.

23. C. Ekman, J. Stenhoff, and B. Dahlbäck, "Gas6 Is Complexed to the Soluble Tyrosine Kinase Receptor Axl in Human Blood," *Journal of Thrombosis and Haemostasis* 8, no. 4 (2010): 838–844, https://doi.org/10.1111/j.1538-7836.2010.03752.x.

24. A. L. Prieto, J. L. Weber, S. Tracy, M. J. Heeb, and C. Lai, "Gas6, a Ligand for the Receptor Protein-Tyrosine Kinase Tyro-3, Is Widely Expressed in the Central Nervous system1," *Brain Research* 816, no. 2 (1999): 646–661, https://doi.org/10.1016/s0006-8993(98)01159-7.

25. L. D. Owlett, B. Karaahmet, L. Le, et al., "Gas6 Induces Inflammation and Reduces Plaque Burden but Worsens Behavior in a Sex-Dependent Manner in the APP/PS1 Model of Alzheimer's Disease," *Journal of Neuroinflammation* 19, no. 1 (2022): 38, https://doi.org/10.1186/s12974-022-02397-y.

26. A. Maimon, V. Levi-Yahid, K. Ben-Meir, et al., "Myeloid Cell–Derived PROS1 Inhibits Tumor Metastasis by Regulating Inflammatory and Immune Responses via IL-10," *Journal of Clinical Investigation* 131, no. 10 (2021): e126089, https://doi.org/10.1172/JCI126089.

27. H. Sadahiro, K. D. Kang, J. T. Gibson, et al., "Activation of the Receptor Tyrosine Kinase AXL Regulates the Immune Microenvironment in Glioblastoma," *Cancer Research* 78, no. 11 (2018): 3002–3013, https://doi.org/10.1158/0008-5472.CAN-17-2433.

28. Y. Yokoyama, E. D. Lew, R. Seelige, et al., "Immuno-Oncological Efficacy of RXDX-106, a Novel TAM (TYRO3, AXL, MER) Family Small-Molecule Kinase Inhibitor," *Cancer Research* 79, no. 8 (2019): 1996–2008, https://doi.org/10.1158/0008-5472.CAN-18-2022.

29. P. L. Hsu, J. Jou, and S. J. Tsai, "TYRO3: A Potential Therapeutic Target in Cancer," *Experimental Biology and Medicine (Maywood, N.J.)* 244, no. 2 (2019): 83–99, https://doi.org/10.1158/1535-7163.MCT-22-0262.

30. A. Mikolajczyk, F. Mitula, D. Popiel, B. Kaminska, M. Wieczorek, and J. Pieczykolan, "Two-Front War on Cancer—Targeting TAM Receptors in Solid Tumour Therapy," *Cancers* 14, no. 10 (2022): 2488, https://doi.org/10.3390/cancers14102488.

31. J. R. Hecht, Y. S. Park, J. Tabernero, et al., "Zanzalintinib Plus Atezolizumab Versus Regorafenib in Refractory Colorectal Cancer (STELLAR-303): A Randomised, Open-Label, Phase 3 Trial," *Lancet (London, England)* 406, no. 10517 (2025): 2360–2370, https://doi.org/10.1016/S0140-6736(25)02025-2.

32. V. Randrian, A. Desette, S. Emambux, et al., "New Artificial Intelligence Score and Immune Infiltrates as Prognostic Factors in Colorectal Cancer With Brain Metastases," *Frontiers in Immunology* 12 (2021): 750407, https://doi.org/10.3389/fimmu.2021.750407.

33. P. Roussille, M. Auvray, D. Vansteene, et al., "Prognostic Factors of Colorectal Cancer Patients With Brain Metastases," *Radiotherapy and Oncology* 158 (2021): 67–73, https://doi.org/10.1016/j.radonc.2021.02.006.

34. A. Desette, P. O. Guichet, S. Emambux, et al., "Deciphering Brain Metastasis Stem Cell Properties From Colorectal Cancer Highlights Specific Stemness Signature and Shared Molecular Features," *Cellular and Molecular Gastroenterology and Hepatology* 16, no. 5 (2023): 757–782, https://doi.org/10.1016/j.jcmgh.2023.07.008.

35. M. O. Hall, M. S. Obin, M. J. Heeb, B. L. Burgess, and T. A. Abrams, "Both Protein S and Gas6 Stimulate Outer Segment Phagocytosis by Cultured Rat Retinal Pigment Epithelial Cells," *Experimental Eye Research* 81, no. 5 (2005): 581–591, https://doi.org/10.1016/j.exer.2005.03.017.

36. M. Karlsson, C. Zhang, L. Méar, et al., "A Single–Cell Type Transcriptomics Map of Human Tissues," *Science Advances* 7, no. 31 (2021): eabh2169, https://doi.org/10.1126/sciadv.abh2169.

37. M. Uhlen, C. Zhang, S. Lee, et al., "A Pathology Atlas of the Human Cancer Transcriptome," *Science* 357, no. 6352 (2017): eaan2507, https://doi.org/10.1126/science.aan2507.

38. J. L. Regan, D. Schumacher, S. Staudte, et al., "Non-Canonical Hedgehog Signaling Is a Positive Regulator of the WNT Pathway and Is Required for the Survival of Colon Cancer Stem Cells," *Cell Reports* 21, no. 10 (2017): 2813–2828, https://doi.org/10.1016/j.celrep.2017.11.025.

39. G. Abboud-Jarrous, S. Priya, A. Maimon, et al., "Protein S Drives Oral Squamous Cell Carcinoma Tumorigenicity Through Regulation of AXL," *Oncotarget* 8, no. 8 (2017): 13986–14002, https://doi.org/10.18632/oncotarget.14753.

40. S. Loges, T. Schmidt, M. Tjwa, et al., "Malignant Cells Fuel Tumor Growth by Educating Infiltrating Leukocytes to Produce the Mitogen Gas6," *Blood* 115, no. 11 (2010): 2264–2273, https://doi.org/10.1182/blood-2009-06-228684.

41. O. Butovsky, M. P. Jedrychowski, C. S. Moore, et al., "Identification of a Unique TGF-β–Dependent Molecular and Functional Signature in Microglia," *Nature Neuroscience* 17, no. 1 (2014): 131–143, https://doi.org/10.1038/nn.3599.

42. N. Aydin, B. Ouliass, G. Ferland, and S. Hafizi, "Modification of Gas6 Protein in the Brain by a Functional Endogenous Tissue Vitamin K Cycle," *Cells* 13, no. 10 (2024): 873, https://doi.org/10.3390/cells13100873.

43. K. V. Myers, S. R. Amend, and K. J. Pienta, "Targeting Tyro3, Axl and MerTK (TAM Receptors): Implications for Macrophages in the Tumor Microenvironment," *Molecular Cancer* 18, no. 1 (2019): 1–14, https://doi.org/10.1186/s12943-019-1022-2.

44. S. K. Smart, E. Vasileiadi, X. Wang, D. DeRyckere, and D. K. Graham, "The Emerging Role of TYRO3 as a Therapeutic Target in Cancer," *Cancers* 10, no. 12 (2018): 474, https://doi.org/10.3390/cancers10120474.

45. M. Tanaka and D. W. Siemann, "Axl Signaling Is an Important Mediator of Tumor Angiogenesis," *Oncotarget* 10, no. 30 (2019): 2887–2898, https://doi.org/10.3390/ijms22189953.

46. J. Hsu, C. Chong, J. Serrill, et al., "Preclinical Characterization of XL092, a Novel Receptor Tyrosine Kinase Inhibitor of MET, VEGFR2, AXL, and MER," *Molecular Cancer Therapeutics* 22, no. 2 (2023): 179–191, https://doi.org/10.1158/1535-7163.MCT-22-0262.

47. B. Garmezy, B. O'Neil, N. J. Shah, et al., "Zanzalintinib (Zanza) + Nivolumab (Nivo) ± Relatlimab (Rela) in Patients (Pts) With Advanced Solid Tumors: Results From Two Dose-Escalation Cohorts of the Phase 1b STELLAR 002 Study," *Journal of Clinical Oncology* 43, no. 16_suppl (2025): 3101, https://doi.org/10.1200/JCO.2025.43.16_suppl.3101.

48. J. J. Miner, B. P. Daniels, B. Shrestha, et al., "The TAM Receptor Mertk Protects Against Neuroinvasive Viral Infection by Maintaining

Blood–Brain Barrier Integrity," *Nature Medicine* 21, no. 12 (2015): 1464–1472, https://doi.org/10.1038/nm.3974.

49. K. Nagata, K. Ohashi, T. Nakano, et al., "Identification of the Product of Growth Arrest-Specific Gene 6 as a Common Ligand for Axl, Sky, and Mer Receptor Tyrosine Kinases," *Journal of Biological Chemistry* 271, no. 47 (1996): 30022–30027, https://doi.org/10.1074/jbc.271.47.30022.

50. R. Akitake-Kawano, H. Seno, M. Nakatsuji, et al., "Inhibitory Role of Gas6 in Intestinal Tumorigenesis," *Carcinogenesis* 34, no. 7 (2013): 1567–1574, https://doi.org/10.1093/carcin/bgt069.

Supporting Information

Additional supporting information can be found online in the Supporting Information section. **Figure S1:** RNAseq data: mRNA expression in normal tissues.